Differential modulation of cell adhesion by interaction between adhesive and counter-adhesive proteins: characterization of the binding of vitronectin to osteonectin (BM40, SPARC)

Sylvia ROSENBLATT*, James A. BASSUK†, Charles E. ALPERS‡, E. Helene SAGE†, Rupert TIMPL§ and Klaus T. PREISSNER*‖

*Haemostasis Research Unit, Kerckhoff Clinic, Max Planck Institute, Sprudelhof 11, D-61231 Bad Nauheim, Federal Republic of Germany, †Department of Biological Structure, School of Medicine, University of Washington, Seattle, WA 98195-7420, U.S.A., ‡Department of Pathology, School of Medicine, University of Washington, Seattle, WA 98195-7420, U.S.A., and §Max-Planck-Institut für Biochemie, Am Klopferspitz 18a, D-82152 Martinsried, Federal Republic of Germany

Heparin-binding forms of vitronectin, a multifunctional adhesive glycoprotein, are associated with the extracellular matrix (ECM) at different locations in the body and serve to promote cell adhesion and the regulation of pericellular proteolysis at sites of angiogenesis. In the present study we characterized the interactions of vitronectin with the counter-adhesive protein osteonectin (also termed SPARC or BM40). Osteonectin and vitronectin were both found associated with the ECM of cultured endothelial cells and were localized in vessel wall sections of kidney tissue. *In vitro*, the heparin-binding multimeric isoform of vitronectin bound to immobilized osteonectin in a saturable manner with half-maximal binding at 30–40 nM. Preincubation of plasma vitronectin with plasminogen activator inhibitor 1 (PAI-1), which provoked multimer formation, induced the binding of vitronectin to osteonectin. Binding was optimal at physiological ionic strength, and binary complexes were stabilized by tissue transglutaminase-mediated cross-linking. In a concentration-dependent fashion, PAI-1, $CaCl_2$, heparin and heparan sulphate, but not other glycosaminoglycans, interfered with the binding of vitronectin to osteonectin. Using vitronectin-derived synthetic peptides as well as mutant forms of recombinant osteonectin, we found that the heparin-binding region of vitronectin interacted with the C-terminal region of osteonectin that contains a high-affinity Ca^{2+}-binding site with counter-adhesive properties. Adhesion of cultured endothelial cells was partly abrogated by osteonectin and was correspondingly reversed by vitronectin in a concentration-dependent manner. These results indicate that specific interactions between vitronectin and osteonectin modulate cell adhesion and might thereby regulate endothelial cell function during angiogenesis.

INTRODUCTION

The extracellular matrix (ECM) is a complex and dynamic structural network that developed as a stabilizing element of all multicellular organisms to ensure their functional integrity and to mediate mechanical forces. The great variability in structure and function of different ECMs is predicted by site-specific biosynthesis of its structural components such as collagens, proteoglycans, elastin, fibronectin and/or laminin. The association of growth factors, proteases and their inhibitors with components of the ECM affords specific modulation of cellular interactions that influence morphogenesis, cell proliferation and differentiation as well as tumour growth and metastasis. The specific induction and repression of gene expression might also be controlled through cellular contacts with the ECM and are required for feedback mechanisms that regulate molecular communications at contact sites between cells and the ECM [1,2].

Most cell–ECM contacts are mediated through adhesion receptors of the integrin and proteoglycan type. Modulation of these interactions during cell migration or cell proliferation involves changes in the pericellular environment. The ECM-associated protein osteonectin (also known as BM40 or SPARC; reviewed in [3]) has been described as a counter-adhesive factor [4] that induces cell rounding and the reorganization of actin stress fibres [5]. Osteonectin is expressed in adult tissues undergoing remodelling and renewal as well as during embryonic development [6], events that are characterized by changes in cell shape and motility. Osteonectin has been shown to alter the expression of matrix protein and protease inhibitor genes, to increase the permeability of endothelial cell monolayers and to modulate growth factor activity [3]. Expression in endothelial cells and modification of osteonectin during pericellular proteolysis have been linked to angiogenesis *in vitro* and *in vivo* [7], in that osteonectin-derived, copper-binding peptides seem to be stimulators of cell proliferation [8]. Osteonectin also binds to collagen type IV [9] and plasminogen, and serves as a cofactor for tissue-type plasminogen activator-mediated plasmin formation [10].

In contrast with osteonectin, the adhesive glycoprotein vitronectin is produced mainly by hepatocytes and is secreted into the circulation. Vitronectin is deposited at various ECM sites in the body, particularly in the vessel wall and the skin and in association with various cancers [11]. From studies with conformation-type monoclonal antibodies and size-exclusion chromatography [12], isoforms of vitronectin in the ECM and in released substances from platelets acquire an altered conformational state with exposed heparin binding and other functional domains and thereby differ from the majority of circulating vitronectin [13,14].

Abbreviations used: DMEM, Dulbecco's modified Eagle's medium; EC module, extracellular module. ECM, extracellular matrix; PAI-1, plasminogen activator inhibitor 1; TBS, Tris-buffered saline.

‖ To whom correspondence should be addressed.

Vitronectin fragments and integrins have been localized to areas of inflammation and angiogenesis [15,16]. Because vitronectin is not produced by vascular cells, the presence of this protein in the vessel wall is best explained by extravasation of heparin-binding forms, as exemplified in the ternary thrombin–antithrombin–vitronectin complex [17–19]. These processes are expected to be accelerated during changes of vascular permeability at sites of angiogenesis [20]. In the subendothelium, vitronectin not only serves major adhesive functions predominantly through interactions with $\alpha_v\beta_3$ integrin but also constitutes the primary binding and stabilizing component for plasminogen activator inhibitor 1 (PAI-1), the major regulator of pericellular proteolysis and fibrinolysis [21]. Moreover, limited proteolysis by plasmin converts vitronectin into a major plasminogen-binding factor of the ECM [22]. Together, these functions of vitronectin are believed to stabilize cell–ECM contacts [23] and facilitate wound healing and repair, e.g. after injury to the vessel wall or during angiogenesis. However, any relationship between adhesive and counter-adhesive components in these processes remains essentially undefined.

In the present report we describe colocalization of vitronectin and osteonectin *in vivo* and define binding characteristics *in vitro*. These studies define molecular details that relate to the apparently opposing effects of vitronectin and osteonectin on adhesive cells. We propose that the binding of vitronectin to osteonectin could lead to changes in adhesive function and thereby contribute to differential morphoregulatory processes in tissues that retain both of these proteins.

MATERIALS AND METHODS

Materials, proteins and antibodies

Collagen type I from calf skin, BSA, tissue transglutaminase, Tween-20, unfractionated heparin (mean molecular mass 12500 Da), heparan sulphate, chondroitin sulphate and dermatan sulphate as well as analytical grade buffer reagents were from Sigma (Munich, Germany) and Roth (Karlsruhe, Germany). The heparinoid pentosan polysulphate was kindly provided by Dr. T. Halse (Benechemie, Munich, Germany). Plasma vitronectin was purified from pooled human plasma as described [24]. The multimeric form of vitronectin was derived by incubation with 6 M urea for 1 h at 37 °C with subsequent dialysis against Tris-buffered saline [20 mM Tris (pH 7.4)/150 mM NaCl] (TBS) to remove urea [12]. The vitronectin–thrombin–antithrombin complex was purified from human serum as described [17] and kindly provided by Dr. H. de Boer (University Hospital, Utrecht, The Netherlands). The monoclonal antibody VN7 was obtained by conventional hybridoma techniques and its characteristics are described elsewhere [12]. Peroxidase-labelled secondary antibodies were purchased from Dako (Hamburg, Germany) and Dianova (Hamburg, Germany). Cell culture medium and supplements were obtained from Gibco (Karlsruhe, Germany). Recombinant human osteonectin, the deletion mutants and the corresponding proteolytic fragments were expressed in HU293 cells and prepared as described [25–27]. The antiserum against human osteonectin was raised as described [9]. Recombinant human osteonectin was also expressed in and purified from *Escherichia coli* as previously described [28,29]. Murine osteonectin-derived synthetic peptides 1.1 (amino acid residues 5–23), 3.2 (154–173) and 4.2 (254–273) are described elsewhere [30]. The vitronectin-derived synthetic peptides VN(341–355) (APRPSLAKKQRFRHR), VN(348–361) (KKQRFRHRNRKGYR), VN(357–370) (RKGYRSQRGHSRGR), VN(366–379) (HSRGRNQNSRRPSR) and VN(371–383) (NQNSRRPSRATWL) were synthesized and analysed as described [22] and were kindly provided by Dr. W. Stüber, Behring Research Laboratories (Marburg, Germany). The synthetic peptides VN(39–51) (CKPQVTRGDVFTM) and VN(52–67) [PQDQY(SO_3^-)TVY(SO_3^-)DDGQQKNN were a gift from Dr. G. Patel (London, U.K.). Recombinant PAI-1, expressed in *E. coli* and isolated in active form as described [31], as well as monoclonal antibody 2C8 against the vitronectin-binding region of PAI-1 [32], was kindly provided by Dr. H. Pannekoek (University of Amsterdam, Amsterdam, The Netherlands). The monoclonal antibodies 12A4 against human PAI-1 and 13H1 against vitronectin were kind gifts of Dr. P. Declerck (University of Leuven, Leuven, Belgium).

Cell culture and adhesion assays

Bovine aortic endothelial cells (less than passage 8) were grown in Dulbecco's modified Eagle's medium (DMEM) with a high glucose concentration and supplemented with 10 % (v/v) fetal bovine serum, 1 % (w/v) penicillin G and 1 % (w/v) streptomycin sulphate. A modification of the procedure of Bassuk et al. (1996) [28] was followed for studies of the inhibition of cell spreading by recombinant osteonectin expressed in *E. coli*. Individual wells of a 24-well tissue culture plastic plate were coated with 2, 5 or 10 μg of human multimeric vitronectin in DMEM at 37 °C. After 3–5 h this medium was removed and replaced with a solution of osteonectin that was dialysed against DMEM containing 1 % penicillin G and 1 % streptomycin sulphate. Solutions with varying amounts of osteonectin in 0.3 ml of DMEM were used. After 15 min at room temperature 0.2 ml of DMEM that contained freshly harvested endothelial cells (2×10^4) was added to each well. Wells that were coated with 5 μg of vitronectin received osteonectin/DMEM with or without 1 % fetal bovine serum. After 2–3 h at 37 °C cultures were photographed with an inverted phase-contrast microscope (Zeiss, Oberkochen, Germany). The degree of cell spreading was quantified by the scoring of three photographic fields, each derived from a well of a triplicate set. Digitized images were obtained from high-resolution scanning of photographic negatives. A 'rounding index' was determined from the formula $I_R = (x+2y+3z)/(x+y+z)$, where x, y and z correspond to the total number of cells in the photographic field [30]. An index of 1 represents completely spread cells, 2 partly spread cells and 3 totally rounded cells.

Binding assays

Binding assays were performed in Maxisorp 96-well plates (Nunc). Osteonectin, its mutants, or collagen type I were coated at a concentration of 5 μg/ml in coating buffer [15 mM Na_2CO_3/35 mM $NaHCO_3$ (pH 9.6)] for 1 h at 37 °C or for 16 h at 4 °C. The wells were blocked with 3 % (w/v) BSA in TBS for 1 h at 22 °C. Subsequently, different forms of vitronectin or the ternary complex (4 μg/ml) were added in TBS containing 0.2 % BSA and 0.1 % Tween-20 in a final volume of 50 μl and were incubated for 2 h at 22 °C. After several washes with TBS containing 0.1 % Tween-20, bound vitronectin was quantified by sequential incubation with the monoclonal antibody VN7 (1.5 μg/ml) for 1 h and with anti-(mouse IgG) conjugated with horseradish peroxidase, diluted in TBS/Tween-20. For colorimetric detection the wells were incubated with 2,2′-azinodi-(3-ethylbenzothiazoline) sulphate(6) and H_2O_2 in 0.1 M sodium acetate/0.05 M NaH_2PO_4 (pH 5.5); absorbance at 414 nm was monitored in a microtitre plate reader (Bio-Rad, Munich, Germany). Increasing final concentrations of NaCl (0–0.8 M) as well as $CaCl_2$ (0–10 mM) were included in the same experimental

protocol as described above. In competition experiments, glycosaminoglycans and synthetic peptides were preincubated with wells for 15 min at twice the final concentration before the measurement of vitronectin binding.

In competition experiments including active PAI-1, 2.5 μg/ml multimeric vitronectin and increasing concentrations of active PAI-1 were mixed in a reaction tube and were incubated for 30 min at 22 °C before being added to the wells coated with osteonectin. Bound multimeric vitronectin was detected as described above. In addition, 1 μg/ml plasma vitronectin and increasing concentrations of active PAI-1 were simultanously added to wells coated with osteonectin or collagen type I and bound vitronectin was detected as described above. Finally, wells coated with osteonectin and collagen type I were incubated with 5 μg/ml PAI-1 and increasing concentrations of plasma vitronectin for 2 h at 22 °C. Bound PAI-1 was detected with the monoclonal antibody 12A4 (1 μg/ml) for 1 h and subsequent incubation with anti-(mouse IgG) conjugated with horseradish peroxidase and substrate. Wells coated with BSA but otherwise treated identically served as controls.

The influence of PAI-1 on the conformational transition of vitronectin was tested by competitive ELISA as previously outlined [12]. Briefly, various concentrations of active PAI-1 were incubated with plasma vitronectin for 1 h at 37 °C followed by reaction with monoclonal antibody 13H1, which recognizes only multimeric vitronectin. In a second step, unbound 13H1 was quantified on vitronectin-coated wells. Moreover, inactivated PAI-1 or active PAI-1 in the presence of anti-PAI-1 monoclonal antibody 2C8 or control antibody were preincubated with plasma vitronectin followed by reaction with biotinylated 13H1 [12] and quantitation was performed accordingly by using streptavidin-conjugated peroxidase.

Immunohistochemistry

Human kidney tissue samples were fixed in Methyl Carnoy's solution (methanol/chloroform), embedded in paraffin and cut into 5 μm thick sections. Sections were blocked by incubation with normal horse serum and reacted with rabbit IgG specific for human vitronectin [24], mouse IgG specific for human osteonectin (Haematologic Technologies, Essex Junction, U.K.), or with irrelevant rabbit antibodies, followed by incubation with secondary antibodies coupled with alkaline phosphatase or horseradish peroxidase respectively. For detection of osteonectin-bound antibody, we used 3,3′-diaminobenzidine with nickel chloride enhancement, whereas for complexes bound to vitronectin we used Vector Red® stain (Vector Laboratories, Burlingame, CA, U.S.A.). Absorption of anti-osteonectin antibody reactivity was achieved by prior incubation with a 10-fold molar excess of human platelet osteonectin for 16 h at 4 °C.

Microscopic fields were recorded on Kodak 100 Ektachrome 35 mm slide film with an Olympus BH2 microscope. Slides were subsequently scanned and archived on a Kodak photographic compact disc and printed on a Tektronix 440 color dye-sublimation printer.

RESULTS

Co-distribution of vitronectin and osteonectin in tissues

The relevance of our study depends on the localization of osteonectin and vitronectin to the same tissue. Immunohistochemical staining of human kidney tissue with antibodies specific for osteonectin and vitronectin revealed that both proteins could be detected in blood vessel walls of the renal cortex. Figure 1 displays histological (Figure 1A) and immunological (Figures 1B to 1E) data for a renal artery with significant levels of osteonectin (dark brown stain) and vitronectin (red stain) in the tunica media. Osteonectin protein is apparent within smooth-muscle cells, whereas vitronectin seems to have a diffuse staining pattern consistent with an extracellular localization (Figures 1D and 1E). The specificity of our anti-osteonectin IgG is demonstrated by absorption with osteonectin protein (compare Figures 1B and 1C). The lack of apparent extracellular immunostaining for osteonectin in Figures 1(D) and 1(E) could be due to (1) a high level of synthesis and a low level of secretion, (2) the rapid turnover of osteonectin [7,8] after secretion that would lead to a loss of immunoreactivity and (3) masking of epitopes by transglutaminase-mediated cross-linking. Similar control studies with vitronectin, anti-vitronectin IgG [16] and irrelevant rabbit IgG indicated that antibodies against vitronectin react in a specific manner.

In the ECM prepared from cultured endothelial cells, strong reactivity of antibodies against both proteins was noted (results not shown). These results indicated to us a possible interaction between osteonectin and vitronectin. We therefore performed direct binding of osteonectin to the vitronectin–thrombin–antithrombin complex, which is found in the subendothelium along the vascular bed and contains conformationally altered (multimeric) vitronectin [17]. The ternary complex exhibited specific binding to immobilized osteonectin and collagen type I (a major vitronectin-binding component of the ECM) (Figure 2). Heparin diminished the interaction with osteonectin as did a vitronectin-derived, heparin-binding synthetic peptide [22]. Incubation of osteonectin and multimeric vitronectin with increasing doses of tissue transglutaminase in solution indicated the stabilization of both proteins by covalent cross-linking. In an enzyme concentration-dependent fashion, comigration of high-molecular-mass bands that were immunoreactive for both proteins was noted on Western blots (results not shown).

Binding of vitronectin to ECM proteins

Binding curves of multimeric and plasma vitronectin to immobilized osteonectin and to collagen type I are shown in Figure 3. The distinct conformational forms of vitronectin exhibited different binding properties: multimeric vitronectin added in increasing concentrations showed saturable binding to both proteins (Figure 3A), with the estimated binding constants (derived from double reciprocal plots) for osteonectin and collagen type I of 33 and 19 nM respectively. In contrast, the binding of plasma vitronectin to collagen type I was about one-quarter to one-fifth as efficient and binding to osteonectin was hardly discernible.

Similar binding assays were also performed at different ionic strengths (Figure 3B). Interaction of multimeric vitronectin with osteonectin reached an optimum at physiological ionic strength (approx. 0.15 M NaCl), whereas binding to collagen type I was optimal under hypotonic conditions and decreased to 50 % of maximum at 0.15 M NaCl. The plasma form of vitronectin exhibited no appreciable binding to osteonectin at any concentration of NaCl, whereas the interaction with collagen type I showed the same dependence on NaCl as multimeric vitronectin, albeit at a lower level. In all cases, binding was decreased to background level at 0.4 M NaCl. These results indicate that the interactions between multimeric vitronectin and osteonectin were mostly ionic in nature, whereas binding to collagen type I was dependent on ionic and non-ionic interactions, in agreement with previous results [33].

The influence of Ca^{2+} ions was tested in subsequent binding experiments. In the presence of increasing concentrations of

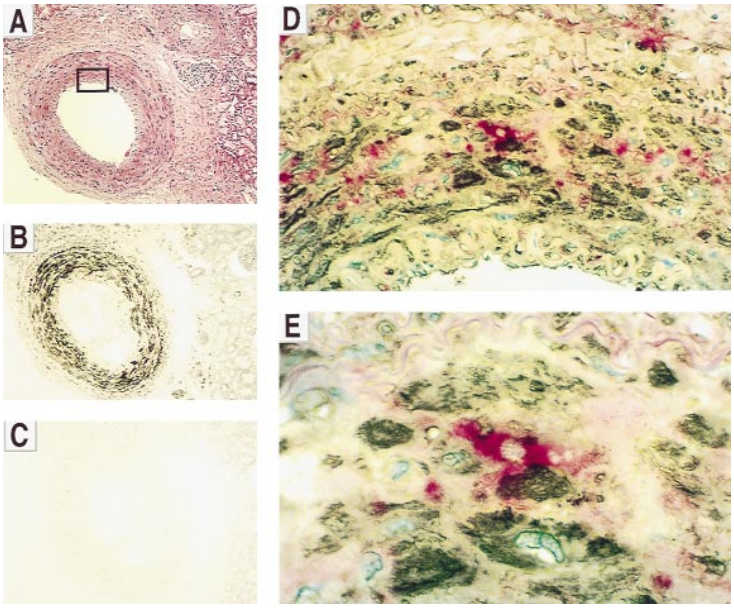

Figure 1 Localization of osteonectin and vitronectin in the neointimal region of a human kidney artery

The tissue sample was derived from an unidentified human patient diagnosed with renal cell carcinoma; shown is a region classified as pathologically normal. All sections used were adjacent. (**A**) Haematoxylin and eosin stain. (**B**) Immunostain for osteonectin. (**C**) Absorption of anti-osteonectin antibody reactivity by prior incubation with a 10-fold molar excess of human platelet osteonectin. (**D**) Double immunostain for osteonectin (dark brown) and vitronectin (red). Shown is an area from the boxed region in (**A**). Counterstaining to visualize cell and tissue edges was performed with Methyl Green. (**E**) Higher magnification of the image in (**D**), in the same orientation. Magnifications: (**A**, **B**) $\times 6.6$, (**C**) $\times 6.6$, (**D**) $\times 26.4$, (**E**) $\times 66$.

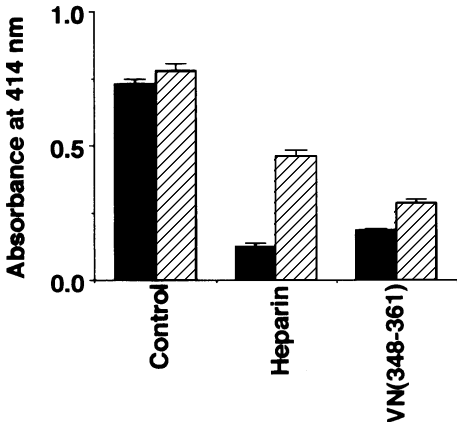

Figure 2 Binding of vitronectin–thrombin–antithrombin complex to osteonectin and collagen type I

Osteonectin (filled bars) and collagen type I (hatched bars) at a concentration of 5 μg/ml were coated on a 96-well plate and incubated with 4 μg/ml isolated ternary vitronectin complex in the absence and in the presence of 10 μg/ml heparin or 1 μg/ml synthetic peptide VN(348–361). Bound vitronectin complex was detected with the monoclonal antibody VN7 against human vitronectin (results are means $\pm$ S.D., $n = 3$).

$CaCl_2$, binding of multimeric vitronectin to osteonectin was gradually inhibited; half-maximal binding was observed at 0.5 mM $CaCl_2$. The interaction of vitronectin with collagen type I was less sensitive to Ca^{2+} ions and exhibited an IC_{50} of 1.2 mM $CaCl_2$ (Figure 3C). These results indicate that low-affinity Ca^{2+}-binding sites of osteonectin and collagen type I interfere with direct binding to multimeric vitronectin. The interactions of plasma vitronectin with collagen type I and osteonectin were not influenced by Ca^{2+} ions (results not shown).

Competition by glycosaminoglycans

From the results shown in Figures 2 and 3, ionic interaction with osteonectin and collagen type I could be mediated mainly by two charged domains in the vitronectin molecule: the negatively charged acidic domain adjacent to the cell-attachment site at the N-terminus and/or the positively charged, basic heparin-binding domain at the C-terminus. Increasing concentrations of heparin interfered with the binding of multimeric vitronectin to osteonectin and to collagen type I and exhibited IC_{50} values of 0.05 and 5 μg/ml respectively (Figure 4A). No difference in binding of plasma vitronectin to collagen type I, with or without heparin, was noted (results not shown). In addition, only heparan sulphate, but not chondroitin sulphate, dermatan sulphate or pentosan polysulphate, was able to block the binding of vitronectin to osteonectin (Figure 4B). Because heparin does not bind to osteonectin (as determined by incubation with biotinylated heparin or by heparin-affinity chromatography; results not shown [34]), the competition by heparin and heparan sulphate was most probably due to the interaction of osteonectin with the heparin-binding site of vitronectin. Moreover, the heparin-binding site of vitronectin seems to be involved in the binding to collagen type I as well, because heparin partly blocked the interaction of both proteins.

Vitronectin is the major PAI-1-binding protein in the ECM; at least two binding sites for PAI-1 in the vitronectin molecule have been identified [13]. One of them is localized upstream of the heparin-binding site [35], which prompted us to investigate the influence of PAI-1 on the binding of vitronectin to osteonectin. In competition assays, active PAI-1 inhibited the interaction between both proteins in a concentration-dependent manner

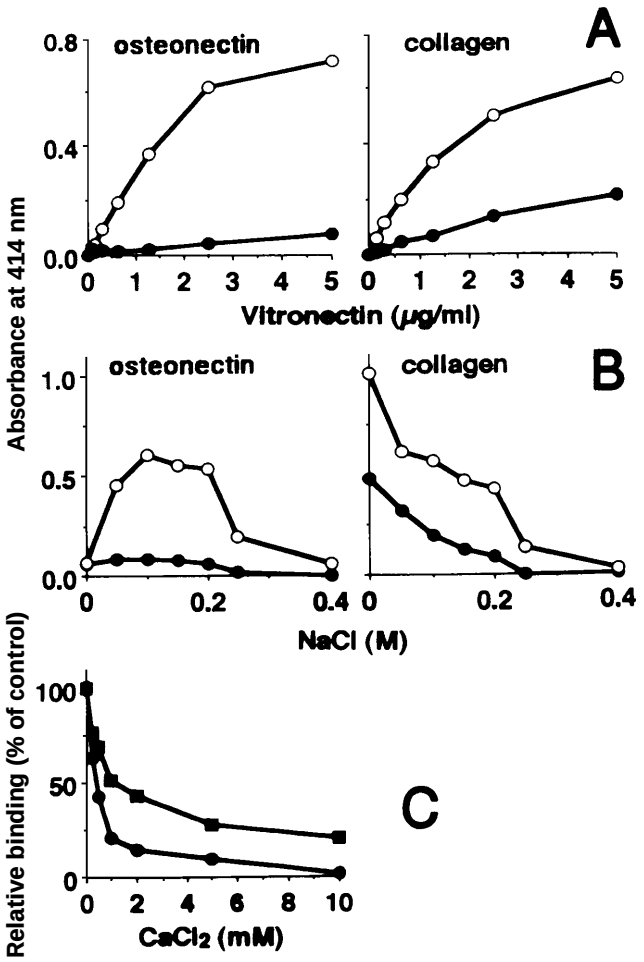

Figure 3 Binding of vitronectin to osteonectin and collagen type I

Osteonectin and collagen type I were immobilized on a 96-well plate, and wells were blocked with 3% (w/v) BSA. (**A**) Various concentrations of plasma vitronectin (●) and multimeric vitronectin (○) were added to the wells, and bound vitronectin was quantified with a monoclonal antibody. (**B**) Osteonectin- and collagen type I-coated wells as indicated were incubated with 2 μg/ml plasma (●) or 2 μg/ml multimeric vitronectin (○) in the presence of various concentrations of NaCl. Bound vitronectin was detected as described above. (**C**) Wells coated with osteonectin (●) and collagen type I (■) were incubated with 2 μg/ml multimeric vitronectin in the presence of various concentrations of $CaCl_2$. Bound vitronectin was detected as described above. The binding of multimeric vitronectin to osteonectin and to collagen type I in the absence of $CaCl_2$ was set at 100%. Results represent duplicate (**A**, **B**) or triplicate (**C**) measurements (variation less than 5%) of experiments repeated at least four times.

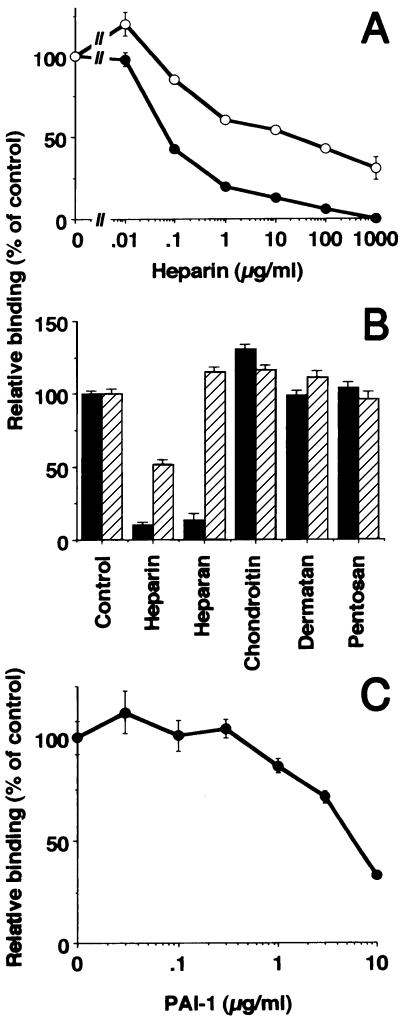

Figure 4 Influence of glycosaminoglycans and PAI-1 on osteonectin–vitronectin interaction

(**A**) Osteonectin (●) and collagen type I (○) were coated on microtitre plates and incubated with 2 μg/ml multimeric vitronectin in the presence of various concentrations of heparin. Detection of bound vitronectin was performed as described above. Control vitronectin binding in the absence of heparin was set at 100%. (**B**) Wells coated with osteonectin (filled bars) or collagen type I (hatched bars) were incubated with 2 μg/ml multimeric vitronectin in the presence of various glycosaminoglycans (heparan, heparan sulphate; dermatan, dermatan sulphate; chondroitin, chondroitin sulphate; pentosan, pentosan polysulphate) (each at 1 μg/ml) and binding was assessed as described above. (**C**) Multimeric vitronectin (2.5 μg/ml) was preincubated with various concentrations of active PAI-1, and the solution was subsequently added to wells coated with osteonectin. Bound multimeric vitronectin was detected as described above. Binding in the absence of PAI-1 was set at 100%. Values represent means ± S.E.M. ($n = 3$) for a typical experiment.

(Figure 4C). However, half-maximal inhibition was reached only at rather high (non-physiological) concentrations of PAI-1.

Identification of binding sites

The role of the heparin-binding site of vitronectin in the described interactions with osteonectin was analysed further by the use of synthetic peptides derived from the acidic N-terminus (residues 39–51 and 52–67) and the basic C-terminus (overlapping sequences between residues 341 and 383) of vitronectin. Only two peptides from the central portion of the heparin-binding region of vitronectin blocked the binding of multimeric vitronectin to both proteins (Table 1). These results confirmed our competition experiments with glycosaminoglycans (Figure 4) and the interpretation that the heparin-binding site of vitronectin might act as major binding site for osteonectin.

Candidate acidic domains in the osteonectin molecule for interaction as complementary site(s) might include Ca^{2+}-binding regions at the N- and C-termini. Osteonectin deletion mutants and proteolytic fragments lacking these sites to various extents were tested in binding assays with multimeric vitronectin as shown in Figure 5. The tryptic fragment T3, which lacks the C-terminal domains III and IV (extracellular module) of osteonectin [9], was minimally bound to multimeric vitronectin, whereas the deletion mutant Δ(8–67) and the proteolytic fragment LE (derived by digestion with leucocyte elastase), which lack different portions

Table 1 Vitronectin binding to osteonectin and collagen type I: competition by vitronectin-derived synthetic peptides

Microtitre wells coated with osteonectin and collagen type I were incubated with 2 μg/ml multimeric vitronectin in the absence (None) or the presence of synthetic peptides (each at 0.2 μg/ml) derived from the vitronectin sequence as indicated. Bound vitronectin was detected by a monoclonal antibody. Control binding in the absence of peptides was set at 100%. Results represent means $\pm$ S.D. ($n = 3$) for four independent experiments.

Peptide	Binding (% of control) to Osteonectin	Collagen type I
None	100	100
VN(39–51)	98.2 $\pm$ 7.1	96.9 $\pm$ 4.0
VN(52–67)	97.4 $\pm$ 7.8	98.0 $\pm$ 1.3
VN(341–355)	63.4 $\pm$ 9.0	81.0 $\pm$ 2.9
VN(348–361)	6.4 $\pm$ 1.6	28.9 $\pm$ 3.4
VN(357–370)	39.2 $\pm$ 2.1	72.5 $\pm$ 4.2
VN(366–379)	79.1 $\pm$ 4.7	95.0 $\pm$ 1.1
VN(371–383)	87.6 $\pm$ 9.1	99.1 $\pm$ 4.5

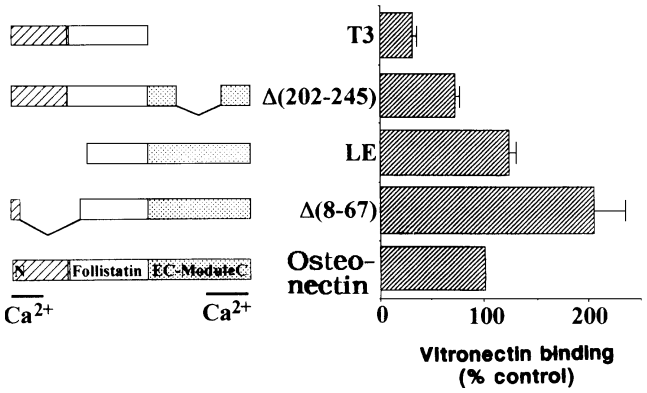

Figure 5 Determination of vitronectin-binding sites in osteonectin

Osteonectin and various deletion mutants [Δ(8–67), Δ(202–245)] or proteolytic fragments (LE, leucocyte elastase fragment; T3, tryptic fragment) were coated on microtitre wells, and binding with 2 μg/ml multimeric vitronectin was performed. Values are expressed relative to the control value representing binding of multimeric vitronectin to osteonectin, which was set at 100%. Results are means $\pm$ S.D. for four independent experiments.

of the N-terminal domain I and parts of domains II or III [26,27], showed even increased binding to vitronectin. The mutant Δ(202–245) with a partial deletion in domain III [27] showed slightly decreased binding compared with that of the intact protein. These results indicate that the major binding site for vitronectin is located in the C-terminus of osteonectin, but that this interaction might also be influenced by its N-terminus. These results are in accordance with the inhibitory effect of $CaCl_2$ on the vitronectin–osteonectin interaction as well. Synthetic peptides representing different functional sites within the protein sequence of osteonectin [30] were included in the competition assay (Table 2). Only peptide 4.2, which represents the C-terminal, Ca^{2+}-binding EF-hand region (domain IV), inhibited binding by more than 70%, whereas peptides 1.1 and 3.2 from the N-terminal (domain I) and the central portion of osteonectin (domain III) had no effect on the interaction between vitronectin and osteonectin.

Table 2 Vitronectin binding to osteonectin: competition by osteonectin-derived synthetic peptides

Immobilized osteonectin was incubated with 2 μg/ml multimeric vitronectin in the absence (None) or the presence of 100 μg/ml osteonectin-derived synthetic peptides 1.1 (5–23), 3.2 (154–173) or 4.2 (254–273). Binding of vitronectin in the absence of peptides was set at 100%. Results represent means $\pm$ S.E.M. ($n = 3$) for a typical experiment.

Peptide	Binding (% of control)
None	100
1.1	87.4 $\pm$ 1.1
3.2	93.4 $\pm$ 0.9
4.2	29.0 $\pm$ 2.0

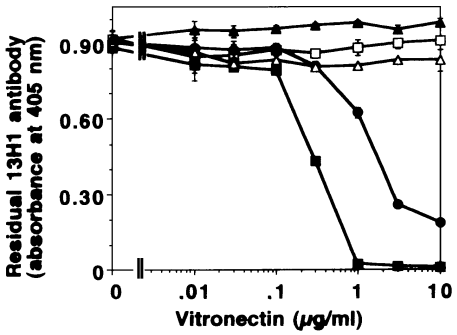

Figure 6 Induction of vitronectin multimers by PAI-1

Equimolar concentrations of plasma vitronectin and active PAI-1 (●), inactive PAI-1 (△) or active PAI-1 preincubated with monoclonal antibody 2C8 (▲) were reacted for 1 h at 37 °C followed by the determination of vitronectin multimers by competitive ELISA as described. The reaction with biotinylated monoclonal antibody 13H1 was performed at various concentrations of vitronectin as indicated. For comparison, plasma vitronectin without additive (□) and preformed multimeric vitronectin (■) were run in parallel in the same assay. Results are means $\pm$ S.D. ($n = 3$) for a typical experiment.

Role of PAI-1 in vitronectin–osteonectin interaction

In addition to their co-localization in the subendothelium, vitronectin, PAI-1 and osteonectin are secretory products released from α-granules during platelet activation/aggregation [10,36]. Moreover, material released from platelets was found to induce the conformational transition from plasma to multimeric vitronectin [12]; we therefore tested the possibility that PAI-1 could be the major component in this conversion reaction. When plasma vitronectin was preincubated with up to equimolar concentrations of active PAI-1, transition into multimeric vitronectin was noted, i.e. as recognized by monoclonal antibody 13H1 [12] (Figure 6), reminiscent of vitronectin multimer formation induced by the thrombin–antithrombin complex [14]. Inactivated PAI-1 or preincubation of active PAI-1 with monoclonal antibody 2C8, which recognizes the vitronectin-binding domain of the inhibitor [32], were ineffective in the induction of multimerization of plasma vitronectin. These results identify PAI-1 as an additional physiological inducer of vitronectin multimerization. Multimers were also discernible as high-molecular-mass products on native polyacrylamide gels when

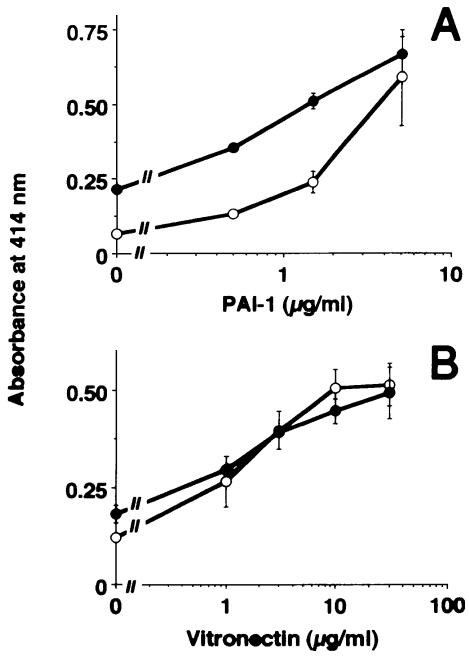

Figure 7 Influence of PAI-1 on binding of vitronectin to osteonectin and collagen type I

(**A**) Vitronectin binding: osteonectin (○) and collagen type I (●) were coated on microtitre wells and were incubated with 1 μg/ml vitronectin in the presence of increasing concentrations of PAI-1 as indicated. Bound vitronectin was detected as described before. (**B**) PAI-1 binding: wells coated with osteonectin (○) and collagen type I (●) were incubated with 5 μg/ml PAI-1 in the presence of increasing concentrations of plasma vitronectin. Solid-phase-bound PAI-1 was quantified with monoclonal antibody. Typical experiments with duplicate measurements are shown (means ± range).

active PAI-1 was added to plasma (H. de Boer, P. G. de Groot, K. T. Preissner, unpublished work).

Although plasma vitronectin hardly bound to osteonectin in the absence of PAI-1 (Figure 7A; see also Figure 3), preincubation with increasing doses of the inhibitor resulted in approx. 10-fold greater vitronectin binding owing to the induction of multimers *in situ*. A similar but weaker effect was observed when vitronectin binding to collagen type I was tested in the presence of active PAI-1. We considered the possibility that ternary complexes were formed between the three interacting components. In a similar ELISA to that described above, increasing doses of plasma vitronectin were added together with active PAI-1 to immobilized osteonectin or collagen type I respectively. In the absence of vitronectin, low specific binding of active PAI-1 to the immobilized proteins was noted, whereas in the presence of vitronectin a 3–5-fold increase in PAI-1 binding was seen (Figure 7B). These results indicate that active PAI-1, as well as vitronectin, is bound to immobilized osteonectin or collagen type I in a ternary complex. The latter two components could thus serve as anchoring sites in the ECM for the PAI-1–vitronectin complex.

Influence of osteonectin–vitronectin interaction on cell adhesion

One prominent feature of osteonectin is its counter-adhesive effect on certain cell types and the prevention of cell spreading, activities which reside in the N- and C-terminal Ca^{2+}-binding domains [28]. Because the aforementioned results indicate direct binding of vitronectin to the C-terminal counter-adhesive site in osteonectin, we tested both proteins in adhesion assays. Endothelial cells plated on surfaces coated with osteonectin hardly attached and showed a rounded morphology, whereas when multimeric vitronectin was bound to osteonectin before cell plating, virtually all cells had attached and/or started to spread (results not shown). Conversely, osteonectin-induced cell rounding of endothelial cells plated on vitronectin was followed quantitatively (Figure 8). The addition of increasing concen-

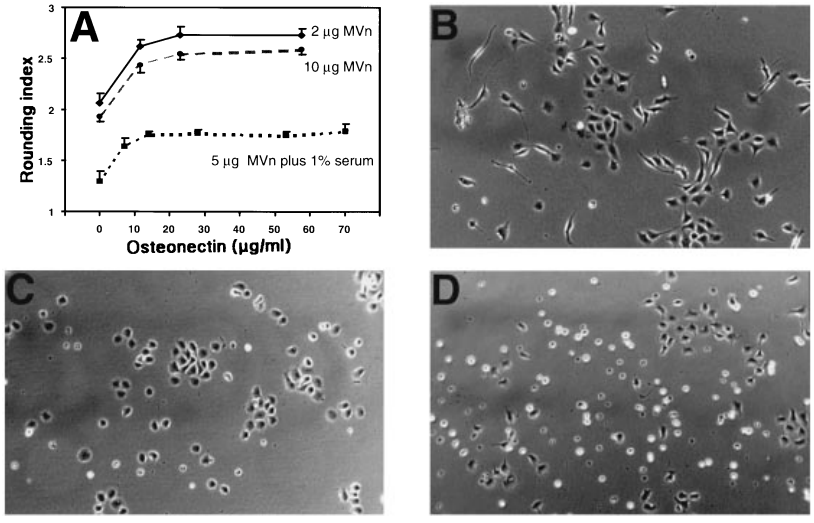

Figure 8 Inhibition of endothelial cell spreading on multimeric vitronectin (MVn) substrate by osteonectin

(**A**) Actively proliferating endothelial cells were tested for their ability to spread on vitronectin-coated tissue plastic dishes in the presence of various concentrations of osteonectin. Dishes were coated with vitronectin at the indicated amounts as described. In some experiments, cells were preincubated for 15 min with osteonectin before addition to the vitronectin-coated well (◆, ●). The lower curve (■) represents experiments in which osteonectin was added to the vitronectin-coated well before the addition of cells; these wells contained a final serum concentration of 1%. Each data point represents the mean ± S.D. for three rounding indices that were calculated from photographs after 2–3 h of incubation. The corresponding data points for the top two curves (2 or 10 μg multimeric vitronectin) are significantly different ($P < 0.01$). An index of 1 represents fully spread cells, 2 partially spread cells and 3 rounded cells. (**B**–**D**) Representative experiment of spreading on 5 μg MVn in the presence of 0 (**B**), 11.5 (**C**) and 23 (**D**) μg/ml recombinant osteonectin in DMEM after 3 h of incubation. Magnification: (**B**–**D**) × 100.

trations of recombinant osteonectin to cells plated on 2, 5 or 10 μg of vitronectin resulted in the progressive loss of cell spreading. These results support the counter-acting functions of vitronectin and osteonectin on cell adhesion.

DISCUSSION

The interaction between cells and the ECM contributes to a number of morphoregulatory events such as tissue remodelling, wound repair and tumour metastasis. Cell behaviour might be altered by the counter-acting function of proteases and their inhibitors in the pericellular space, by deposition or release of growth factors in the ECM, or by modification of its composition with respect to adhesive properties. Of growing interest are proteins exhibiting counter-adhesive properties for cells, such as osteonectin (also designated SPARC or BM40), tenascin C and thrombospondin-1, recently termed 'matricellular' proteins [37]. Although the underlying mechanisms for their counter-adhesive properties remain unclear, the following possibilities could account for repulsive activity: (1) direct competition with adhesion proteins for cellular receptors that mediate cell anchorage and spreading; (2) disintegration of ECM, which leads to the prevention of adhesion receptor clustering; (3) the direct interaction of cell surface receptors [38] with counter-adhesive domains (localized to a Ca^{2+}-binding domain in osteonectin [30] or to heparin-binding regions in thrombospondin-1 [39]); and/or (4) modulation of the pericellular environment by interference with anti-proteolytic events that stabilize adhesive interactions. As we have demonstrated in this report, direct interaction between osteonectin and the adhesion protein vitronectin could account for mutual neutralization of their biological functions and for modulation of pericellular proteolysis.

Localization of both components was recognized in vascular walls in various tissues, particularly in the kidney. In addition, osteonectin and vitronectin are found together as platelet secretory products at sites of vascular injury [3,13]. A direct molecular relationship between osteonectin and vitronectin was established by direct binding experiments. We could demonstrate the high-affinity association of osteonectin predominantly with multimeric vitronectin, the molecular form of the adhesion protein present in the ternary complex, secreted from platelets and present in the ECM. From competition studies with basic vitronectin-derived peptides, heparin and heparan sulphate, we identified the heparin-binding site of multimeric vitronectin as an essential region for interaction with osteonectin. In contrast, plasma vitronectin, in which this site is cryptic, displayed virtually no binding. This result indicates that the conformational transition of plasma vitronectin to the osteonectin binding form is required. This contention was supported by the direct binding of osteonectin to the ternary vitronectin–thrombin–antithrombin complex, which constitutes the major circulating heparin-binding form of vitronectin [17].

The complementary binding site(s) on osteonectin seem(s) to be more complex. That interactions with vitronectin could be inhibited by salt concentrations greater than 0.2 M and by Ca^{2+} ions (0.5–1 mM) indicates the involvement of Ca^{2+}-binding acidic domain(s) of osteonectin. Together with the binding results obtained with osteonectin mutants and synthetic peptides, the most recent model of osteonectin favours the C-terminus as major vitronectin-binding site [40,41]. The flexible N-terminal region (domain I; 54 residues) is polyanionic owing to several glutamic acid residues and binds Ca^{2+} with low affinity (K_d approx. 5–10 mM) [27]. It is followed by the follistatin-like module (approx. 100 residues) and the C-terminal domain III (approx. 130 residues), which represents a novel Ca^{2+}-binding extracellular (EC) module. X-ray crystallography of the EC module of osteonectin demonstrated the presence of a pair of EF-hands that can be occupied by two Ca^{2+} ions [41] with estimated K_d values of 0.1 μM and 0.5 mM ([27,40], and unpublished observations). Because the C-terminal, second EF-hand high-affinity site remains saturated under our experimental conditions [27], the first EF-hand Ca^{2+}-binding site of moderate affinity could be responsible for the observed inhibition by Ca^{2+}. This result was consistent with the studies demonstrating that the complete or partial removal of domains III and IV (EC module) or a synthetic EF-hand decreased the binding of osteonectin to vitronectin. The complete or partial deletion of domain I, however, enhanced binding, despite the fact that its acidic properties would make it a good candidate for interactions with the heparin-binding site of vitronectin. It is likely that conformational changes in osteonectin due to the internal binding of domain I to the C-terminal portion affect interaction with vitronectin.

The fact that multimeric form of vitronectin rather than the circulating plasma form predominantly binds to osteonectin indicates that these interactions are preferentially taking place within the ECM environment rather than in the soluble phase. Because PAI-1 is also found at vitronectin-rich sites of the ECM, it has been proposed that vitronectin–PAI-1 complexes, which are unequivocally identified in plasma [42], might also become immobilized within the ECM [35,43]. It is still unclear, however, whether these complexes in the ECM differ from the soluble ones and how multimerization of vitronectin is induced in the absence of blood clotting. Here we demonstrate that active PAI-1 is able to induce directly the conformational transition from plasma to multimeric vitronectin and that contact with the vitronectin-binding site of PAI-1 is required because the monoclonal antibody 2C8 (which covers this epitope [32]) prevented the PAI-1 inducing effect. Moreover, PAI-1 invokes osteonectin binding to the multimeric adhesive protein. These findings are reminiscent of earlier observations in which multimeric forms of vitronectin were identified in material released from platelets, which is a rich source of active PAI-1 [12]. Moderate binding of PAI-1 to osteonectin and collagen type I was also observed that increased substantially in the presence of vitronectin, implying the possible formation of ternary complexes.

Our results also help to clarify contradicting interpretations about different binding sites of vitronectin for PAI-1: the observed proteolysis of ECM by plasmin, which releases active PAI-1 and correlates with the degradation of the heparin-binding site of vitronectin [22,35], is compatible with an adapter function of the adhesion protein as proposed in the present paper. Although proteolysis of the heparin-binding site does not destroy the primary PAI-1-binding site in vitronectin, which resides in the N-terminal 'somatomedin-B' domain [44], this treatment apparently dissociates the interaction between vitronectin and osteonectin or collagen type I. At the expected concentrations of these components in an ECM environment, we propose that (1) vitronectin–PAI-1 complexes are linked to osteonectin/collagen type I-rich sites; (2) the latter two components might serve as complementary PAI-1-binding proteins; (3) variations in the composition or proteolysis of the described proteins might influence cell–matrix interactions. Additional observations also indicate that PAI-1 itself might have a major impact on the motility of cells [44a].

Additional support for these propositions came from cell adhesion experiments on mixed osteonectin/vitronectin substrata. Owing to specific binding of vitronectin, the counter-adhesive function of osteonectin was greatly neutralized, as evidenced by quantitative cell-rounding evaluation. The strongest

counter-adhesive activity of osteonectin co-localizes within the Ca^{2+}-binding region of the molecule, which was identified as a vitronectin-binding site: the cell-repulsive function of osteonectin might therefore become masked. Indeed, immobilized osteonectin can maintain cells as attached but round for several hours, whereas vitronectin directly promotes adhesion and spreading of endothelial cells as soon as it is allowed to bind to osteonectin (results not shown). A prominent counter-adhesive activity of exogenously added osteonectin [5] on cells adherent to vitronectin was also seen. From preliminary experiments we can exclude the possibility that direct competition of osteonectin for vitronectin binding to integrins is responsible for the counter-adhesive function of the Ca^{2+}-binding protein (S. Rosenblatt and K. T. Preissner, unpublished work). Nevertheless, cellular receptors for osteonectin might account for the transmission of its counter-adhesive function in a direct or indirect manner [38].

With regard to pericellular proteolysis, we offer an additional possibility for the counter-adhesive function of osteonectin and its modulation by vitronectin. At high PAI-1 concentrations we could demonstrate that complex formation with the inhibitor prevents the binding of vitronectin to osteonectin. Together with a possible cofactor function of osteonectin for tissue plasminogen activator-mediated plasmin formation [10], additional functional consequences for pericellular proteolysis could result whether or not osteonectin is in a complex with vitronectin, because osteonectin might serve a PAI-1 binding function as well. In addition, recent results also indicate that urokinase receptor, as a novel vitronectin-binding protein on endothelial cells, can modulate cellular contacts without the action of plasmin [45]. Because PAI-1 can block the binding of vitronectin to the urokinase receptor [45], in this system the inhibitor modulates the binding of several macromolecular components to vitronectin. Our observations indicate a novel relationship between adhesive and counter-adhesive components of the ECM and could be relevant for the fine-tuning of cellular contacts in several biological systems.

We thank Thomas Schmidt and Kelly Hudkins-Loya for skilful technical assistance. This publication is part of a thesis by S.R. at the Biological Faculty, Justus-Liebig-Universität, Giessen, Germany. This work was supported by a grant (Pr 327/1-2) from the Deutsche Forschungsgemeinschaft (Bonn, Germany), by a grant from the University of Washington Royalty Research Fund and by National Institues of Health grants GM 40711 and DK 47659.

REFERENCES

1 Lin, C. Q. and Bissell, M. J. (1993) FASEB J. **7**, 737–743
2 Raghow, R. (1994) FASEB J. **8**, 823–831
3 Lane, T. F. and Sage, E. H. (1994) FASEB J. **8**, 163–173
4 Sage, H., Vernon, R. B., Funk, S. E., Everitt, E. A. and Angello, J. (1989) J. Cell Biol. **109**, 341–356
5 Murphy-Ullrich, J. E., Lane, T. F., Pallero, M. A. and Sage, E. H. (1995) J. Cell. Biochem. **57**, 341–350
6 Sage, H., Vernon, R. B., Decker, J., Funk, S. and Iruela-Arispe, M. L. (1989) J. Histochem. Cytochem. **37**, 819–829
7 Iruela-Arispe, M. L., Lane, T. F., Redmond, D., Reilly, M., Bolender, R. P., Kavanagh, T. J. and Sage, E. H. (1995) Mol. Biol. Cell **6**, 327–343
8 Lane, T. F., Iruela-Arispe, M. L., Johnson, R. S. and Sage, E. H. (1994) J. Cell Biol. **125**, 929–943
9 Mayer, U., Aumailley, M., Mann, K., Timpl, R. and Engel, J. (1991) Eur. J. Biochem. **198**, 141–159
10 Kelm, R. J., Swords, N. A., Orfeo, T. and Mann, K. G. (1994) J. Cell Biol. **269**, 30147–30153
11 Dahlbäck, K., Löfberg, H. and Dahlbäck, B. (1986) Acta Derm. Venereol. **66**, 461–467
12 Stockmann, A., Hess, S., Declerck, P., Timpl, R. and Preissner, K. T. (1993) J. Biol. Chem. **268**, 22874–22882
13 Preissner, K. T. (1991) Annu. Rev. Cell Biol. **7**, 275–310
14 Tomasini, B. R. and Mosher, D. F. (1990) Prog. Hemostas. Thromb. **10**, 269–305
15 Kramer, M. D., Gissler, H. M., Weidenthaler-Barth, B. and Preissner, K. T. (1993) in Biology of Vitronectins and their Receptors (Preissner, K. T., Rosenblatt, S., Kost, C., Wegerhoff, J. and Mosher, D. F., eds.), pp. 295–301, Elsevier, Amsterdam
16 Casaroli Marano, R. P., Preissner, K. T. and Vilaro, S. (1995) Exp. Eye Res. **60**, 5–17
17 de Boer, H. C., Preissner, K. T., Bouma, B. N. and de Groot, P. G. (1995) J. Biol. Chem. **270**, 30733–30740
18 Hess, S., Kanse, S. M., Kost, C. and Preissner, K. T. (1995) Thromb. Haemostas. **74**, 258–265
19 Völker, W., Hess, S., Vischer, P. and Preissner, K. T. (1993) J. Histochem. Cytochem. **41**, 1823–1832
20 Senger, D. R. (1996) Am. J. Pathol. **149**, 1–7
21 Mimuro, J. and Loskutoff, D. J. (1989) J. Biol. Chem. **264**, 936–939
22 Kost, C., Stüber, W., Ehrlich, H., Pannekoek, H. and Preissner, K. T. (1992) J. Biol. Chem. **267**, 12098–12105
23 Ciambrone, G. J. and McKeown-Longo, P. J. (1990) J. Cell Biol. **111**, 2183–2195
24 Preissner, K. T., Wassmuth, R. and Müller-Berghaus, G. (1985) Biochem. J. **231**, 349–355
25 Nischt, R., Pottgiesser, J., Krieg, T., Mayer, U., Aumailley, M. and Timpl, R. (1991) Eur. J. Biochem. **200**, 529–536
26 Maurer, P., Mayer, U., Bruch, M., Jenö, P., Mann, K., Landwehr, R., Engel, J. and Timpl, R. (1992) Eur. J. Biochem. **205**, 233–240
27 Pottgiesser, J., Maurer, P., Mayer, U., Nischt, R., Mann, K., Timpl, R., Krieg, T. and Engel, J. (1994) J. Mol. Biol. **238**, 563–574
28 Bassuk, J. A., Baneyx, F., Vernon, R. B., Funk, S. E. and Sage, E. H. (1996) Arch. Biochem. Biophys. **325**, 8–19
29 Bassuk, J. A., Braun, L. P., Motamed, K. and Sage, E. H. (1996) Int. J. Biochem. Cell Biol. **9**, 1031–1043
30 Lane, T. F. and Sage, E. H. (1990) J. Cell Biol. **111**, 3065–3076
31 Sancho, E., Tonge, D. W., Hockney, R. C. and Booth, N. A. (1994) Eur. J. Biochem. **224**, 125–134
32 van Meijer, M., Klein Gebbink, R., Preissner, K. T. and Pannekoek, H. (1994) FEBS Lett. **352**, 342–346
33 Gebb, C., Hayman, E. G., Engvall, E. and Ruoslahti, E. (1986) J. Biol. Chem. **261**, 16698–16703
34 Sage, E. H., Johnson, C. and Bornstein, P. (1984) J. Biol. Chem. **259**, 3993–4007
35 Preissner, K. T., Grulich-Henn, J., Ehrlich, H. J., Declerck, P., Justus, C., Collen, D., Pannekoek, H. and Müller-Berghaus, G. (1990) J. Biol. Chem. **265**, 18490–18498
36 Preissner, K. T., Holzhüter, S., Justus, C. and Müller-Berghaus, G. (1989) Blood **74**, 1989–1996
37 Bornstein, P. (1995) J. Cell Biol. **130**, 503–506
38 Yost, J. C. and Sage, E. H. (1993) J. Biol. Chem. **268**, 25790–25796
39 Murphy-Ullrich, J. E., Gurusiddappa, S., Frazier, W. A. and Höök, M. (1993) J. Biol. Chem. **268**, 26784–26789
40 Maurer, P., Hohenadl, C., Hohenester, E., Göhring, W., Timpl, R. and Engel, J. (1995) J. Mol. Biol. **253**, 347–357
41 Hohenester, E., Maurer, P., Hohenadl, C., Timpl, R., Jansonius, J. N. and Engel, J. (1996) Nature Struct. Biol. **3**, 67–73
42 Declerck, P. J., De Mol, E., Alessi, M.-C., Baudner, S., Paques, E.-P., Preissner, K. T., Müller-Berghaus, G. and Collen, D. (1988) J. Biol. Chem. **263**, 15454–15461
43 Mimuro, J. and Loskutoff, D. J. (1989) J. Biol. Chem. **264**, 936–939
44 Seiffert, D., Ciambrone, G., Wagner, N. V., Binder, B. R. and Loskutoff, D. J. (1991) J. Biol. Chem. **269**, 2659–2666
44a Kjoller, L., Kanse, S. M., Kirkegaard, T., Rodenburg, K. W., Ronne, E., Goodman, S. L., Preissner, K. T., Ossowski, L. and Andreasen, P. A. (1997) Exp. Cell Res. **232**, 319–328
45 Kanse, S. M., Kost, C., Wilhelm, O. G., Andreasen, P. A. and Preissner, K. T. (1996) Exp. Cell Res. **224**, 344–353

Received 24 October 1996/13 January 1997; accepted 22 January 1997